

Rheology of Giant Vesicles: A Micropipette Study

N. Fa, C. M. Marques, E. Mendes,* and A. P. Schröder

LDfC-CNRS UMR 7506, 4 rue Blaise Pascal, 67070 Strasbourg Cedex, France

(Received 16 June 2003; published 10 March 2004)

We develop a micropipette rheometer to study the effect of oscillatory shear flow on the spontaneous fluctuations of phospholipid bilayers. Our results on giant vesicles show that oscillatory shear flow leads to a suppression of membrane fluctuations. They also imply that the Helfrich equation is modified in the presence of the flow. This equation, a fundamental constitutive relation between the amount of area stored in the fluctuations and the membrane tension, must be supplemented under oscillatory shear by a flow excess function that we determine.

DOI: 10.1103/PhysRevLett.92.108103

PACS numbers: 87.15.Ya, 05.70.Np, 68.03.Cd, 87.16.Dg

Fluid bilayers are prevalent in many natural and industrial colloidal suspensions [1]. Self-assembled from phospholipids and other surfactant solutions, they build in the biological realm the walls of liposomes and cells [2]. In cosmetics, pharmaceuticals, or detergency, formulations of membrane solutions not only allow for the transport and release control of other chemical constituents such as drugs and scents but also help to control solution stability and flow properties [3,4]. The behavior of fluid bilayers in quiescent solutions is now well understood. Following seminal work by Helfrich [5] who first recognized the importance of the membrane bending elasticity, extensive theoretical and experimental studies contributed to the writing of one of the finest chapters in modern statistical physics of soft condensed matter [6]. Surprisingly, much less is known about the physics of single bilayers under flow, in spite of the ubiquitous presence of flow fields when membrane systems are formulated, conditioned, transported, and employed. In this Letter we report for the first time a measure of the flow effect on the Helfrich equation, the fundamental constitutive relation of fluid bilayers. This relation states that, although bilayers self-assemble from solution and should as such be tensionless objects, thermal fluctuations require some of the available membrane surface, thus reducing the projected area and generating tension. The Helfrich equation, connecting the relative excess area and the membrane tension, reads in the absence of flow

$$\frac{A - A^a}{A^a} = \frac{k_B T}{8\pi k_c} \ln \left[\frac{\sigma_0}{\sigma} \right], \quad (1)$$

where A is the actual area, A^a the apparent, projected area [5,7], k_c a membrane material parameter describing the bending elasticity, σ the actual tension on the membrane and σ_0 some fixed, reference value for the tension [8]. A micropipette apparatus first developed by Evans [9] exploits this relation for giant vesicles, large enough (10–100 μm) to be studied in the optical range. In this geometry, sketched in Fig. 1, a cylindrical pipette of internal radius r holds the vesicle with some pressure difference ΔP . The vesicle, originally in a spherical shape of radius R_0 , acquires also a cylindrical component of

length $L - r$ and a hemispherical cap of radius r . These geometric quantities and the Laplace law [10] allow a simple test of Eq. (1). One usually plots the relative excess area *difference* $\alpha = (A^a - A_0^a)/A_0^a$ as a function of the measured tension σ , where A_0^a is the optically measured surface at some initial value of the tension and A^a is the optically measured surface for consecutive tension values σ . The linearity of the $[\alpha, \log \sigma]$ plot confirms the validity of the Helfrich relation and provides an operational method for extracting the value of the bending modulus k_c from the plot slope, as will be shown below.

We study the effect of flow on the Helfrich Eq. (1) by developing a micropipette rheometer (MpR), sketched in Fig. 1. The vesicle is held by a micropipette under a pressure difference ΔP , above a flat, fixed surface. A second flat surface, of lateral dimensions much larger than the vesicle, is held parallel to the bottom surface, at a distance e . Lateral movement of this surface with amplitude ϵ and frequency f creates an oscillatory flow field in the gap characterized by some shear rate $\dot{\gamma}$. We will show below that the vesicle behavior under the flow stress can be well described by a modified Helfrich

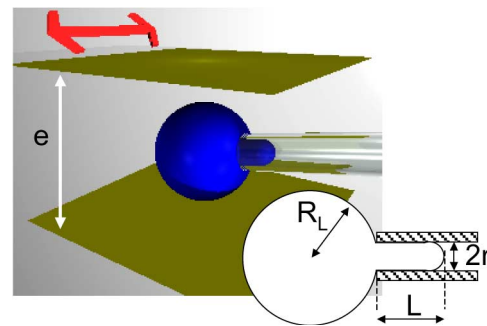


FIG. 1 (color online). A typical experimental configuration for a micropipette rheometer. The vesicle of initial diameter $2R_0$ is held close to the bottom surface by the suction of the micropipette. The membrane is sucked into the micropipette acquiring the geometry of a cylinder capped by a hemisphere. The distance from the micropipette tip to the hemisphere top is L , and the internal diameter is $2r$. The top surface moves perpendicular to the micropipette axis.

relation of the form

$$\frac{A - A^a}{A^a} = \frac{k_B T}{8\pi k_c} \ln \left[\frac{\sigma_0}{\sigma} \right] + F(\dot{\gamma}, \sigma). \quad (2)$$

In the following, we discuss the structure of the flow excess function $F(\dot{\gamma}, \sigma)$ after describing the main aspects of the micropipette rheometer and the associated experimental conditions.

Giant vesicles were prepared by the electroformation method [11]. The 1,2-Dioleoyl-sn-glycero-3-phosphocholine (DOPC) phospholipids were purchased from Avanti and used without further purification. A chloroform solution of DOPC at 0.2 mg ml^{-1} was then spread on a ITO covered glass and dried under vacuum for 10 h. A second identical glass plate was used to cover an incubation chamber delimited by a ring of Sigillum wax (Vitrex, Copenhagen, Denmark) and filled with a 0.1 M solution of sucrose. An ac voltage of 5 V and 10 Hz was applied across the 1 mm chamber gap for about 3 h. The vesicles were then transferred into the observation chamber filled with a glucose solution of 0.102 M. The slight density difference between the inner and outer solutions drive the vesicles to the neighborhood of the bottom plate where they can easily be handled and observed. The concentrations of glucose and sucrose osmotically match the inner and outer solutions, and avoid swelling or deswelling of the vesicles. Images are obtained by a Nikon inverted microscope Eclipse TE200, with a charge-coupled device Hamamatsu C5405 camera. A micropipette driven by a xyz shaft of $1 \mu\text{m}$ precision is brought into contact with a chosen vesicle, and then a pressure difference is applied through a hydraulic system [12]. The measurement by a liquid-liquid pressure transducer (DP103-08, Validyne, SEI3D, USA) allows for a pressure precision of 10^{-2} Pa.

In the absence of flow, the MpR reproduces classical results from a micropipette apparatus. Micropipettes are prepared with an internal radius close to $5 \mu\text{m}$. Pressure increments of at least $\Delta P = 0.03 \text{ Pa}$ are applied to the vesicle, leading to a corresponding increase of the total length L of the vesicle drawn into the micropipette. Because the total volume enclosed by the vesicle remains constant throughout our experiments, the value of the relative excess area difference is given by $\alpha = (R_L^2 + rL/4)/R_0^2 - 1$, where R_0 is the radius of the free vesicle, R_L is the outer radius of the vesicle given by volume conservation $R_L^3 = R_0^3 - r^3/4 - 3r^2L/4$, and other quantities have been defined above. Similarly, the value of the tension is given by $\sigma = \Delta P/2 \times r/(1 - r/R_L)$. As expected, in the absence of flow, there is a linear relationship between the logarithm of the tension and the relative excess area difference α . We performed similar experiments for a series of 15 different vesicles, obtaining an average value for the bending modulus $k_c = 22 \pm 3k_B T$, close to values reported in the literature [13]. In practice, the Helfrich relation is obeyed only in a finite range of the

tension, corresponding typically in our experiments to α values in the range $[0, 0.03]$. Above a certain value, most of the excess surface has been consumed, and one starts to stretch the actual membrane, deviating from the fluctuation logarithmic region of the $\alpha(\sigma)$ curve. All the experiments described below were performed in the fluctuation regime.

As explained above, the MpR was designed to measure flow field effects on the vesicle behavior. The flow is imposed by the movement of the upper plate, parallel to the lower surface and perpendicular to the micropipette axis — see Fig. 1. The upper plate is a rectangular glass slide of dimensions $5 \times 5 \times 0.17 \text{ mm}^3$, driven by a piezoelectric actuator PiezoJena PX400, coupled to a function generator Agilent 33120-A. Typical experiments are performed by imposing an oscillatory motion of the form $\epsilon(t) = \epsilon_0 \sin(2\pi f t)$, with amplitudes ϵ_0 and frequencies f in the ranges $0.7 < \epsilon_0 < 5 \mu\text{m}$ and $0.1 < f < 10 \text{ Hz}$. Also, the distance e between the upper and the bottom plates, fixed during an experiment, is typically in the range $0.5 < e < 2 \text{ mm}$. Note that in the absence of a vesicle, a pure shear flow is generated far from the plate borders, with a flow velocity profile $v_x = \dot{\gamma}(t)y$, where the coordinate system (x, y, z) has its z axis parallel to the micropipette axis, and x is in the bottom plate. Such flow is characterized by a single quantity, the shear rate $\dot{\gamma}(t)$ that is a combination of amplitude, frequency, and gap thickness, $\dot{\gamma}(t) = \dot{\gamma} \cos(2\pi f t)$, with $\dot{\gamma} = 2\pi f \epsilon_0/e$ [14]. Under typical conditions, shear rates span the range $10^{-4} < \dot{\gamma} < 10^{-1} \text{ Hz}$.

The MpR can be operated in several different modes that we now describe. In the fixed pressure mode, an initial suction pressure is applied to the vesicle in the absence of flow and then kept constant under flow. The suction pressure is low, typically of the order of 0.03 to 0.1 Pa, well within the fluctuation regime. Under an oscillatory flow, the length L of the vesicle section inside the micropipette increases. A modification of the flow conditions imposed by a new chosen amplitude or frequency is followed by relaxation in a few seconds towards a new L value. Such modifications are reversible; an amplitude or frequency cycle allows one to recover consistent, path independent L values. As shown in Fig. 2(a), the relative excess area difference α increases linearly with the shear amplitude ϵ_0 when the shear frequency f is kept constant, and with f at fixed ϵ_0 . The linear dependence holds as far as the associated α values stay within the fluctuation regime. We investigated the behavior of many different vesicles, choosing for this particular set of experiments $0.75 < \epsilon_0 < 5 \mu\text{m}$, $0.1 < f < 10 \text{ Hz}$, $e = 1 \text{ mm}$, and $e = 2 \text{ mm}$. Anticipating a key role for the shear rate, we display in Fig. 2(b) the values of the slope $\Lambda = \partial\alpha/\partial\dot{\gamma}$ for all the performed experiments. We stress at this point that each experiment is performed with a different vesicle, and the dispersion of slope values reflects thus a dispersion in some constitutive parameter of the vesicle. We return later to this issue.

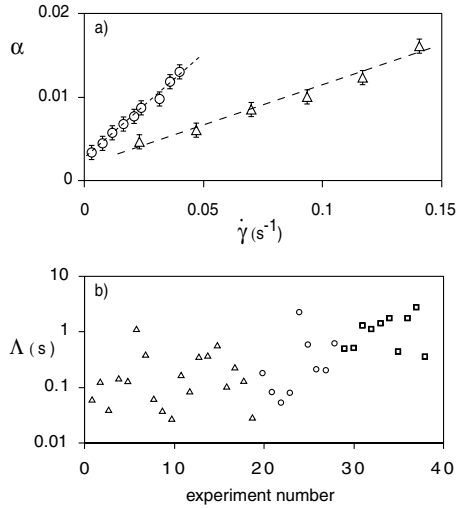


FIG. 2. (a) Results for the increase of the relative excess area difference in the presence of an oscillatory shear gradient of amplitude $\dot{\gamma}$. (b) Distribution of the slope values $\Lambda = \partial\alpha/\partial\dot{\gamma}$ for different experiments. (Δ) fixed amplitude, (\square) fixed frequency, (\circ) fixed amplitude, movement along the micropipette axis.

A second mode of operation for the micropipette rheometer allows for performing the usual suction experiment under dynamic conditions. For each experiment, the vesicle is grabbed by the micropipette in the presence of the flow, and then the suction increased as previously described for quiescent conditions. We display in Fig. 3(a) two suction experiments performed with amplitude $\epsilon_0 = 0.45 \mu\text{m}$, at a fixed distance $e = 1000 \pm 5 \mu\text{m}$ from the bottom plate, with frequencies corresponding to shear rates $\dot{\gamma} = 2.4 \times 10^{-3} \text{ Hz}$ and $\dot{\gamma} = 3.3 \times 10^{-3} \text{ Hz}$. An experiment in quiescent conditions is also shown for comparison. As the figure shows, in the presence of flow, the pressure displacement curve still follows a logarithmic law but with a different slope that is shear rate dependent. One can thus, for each shear rate, determine an apparent curvature modulus $k_c(\dot{\gamma})$. We performed a series of experiments in the shear rate range 7×10^{-4} to $4 \times 10^{-2} \text{ Hz}$. Values for the effective modulus $k_c(\dot{\gamma})$ are shown in Fig. 3(b) where each point is an average over 5–13 different vesicles. The experimental values are well described by a function of the form

$$k_c(\dot{\gamma}) = \frac{k_c(0)}{1 + \tau_0 \dot{\gamma}} \quad (3)$$

as shown by the linearity of the curve, when we plot $k_c(0)/k_c(\dot{\gamma})$ as a function of $\dot{\gamma}$, with $k_c(0) = 22k_B T$. The best fit gives $\tau_0 = 143 \text{ s}$. The linear dependence of the relative excess area difference α with the shear rate, shown in Fig. 2(a), the existence of an apparent modulus, and its functional from Eq. (3) imply a flow contribution to the Helfrich relation (2) of the form

$$F(\dot{\gamma}, \sigma) = \tau_0 \dot{\gamma} \frac{k_B T}{8\pi k_c} \ln \left[\frac{\sigma_1}{\sigma} \right] \quad (4)$$

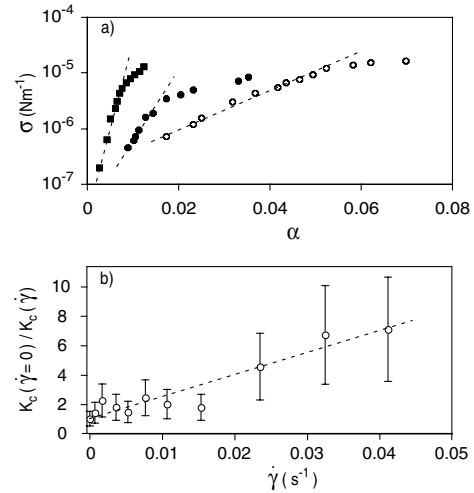


FIG. 3. (a) Results for suction experiments at fixed shear rate: (\blacksquare) $\dot{\gamma} = 0 \text{ s}^{-1}$, (\bullet) $\dot{\gamma} = 2.4 \times 10^{-3} \text{ s}^{-1}$, and (\circ) $\dot{\gamma} = 3.3 \times 10^{-3} \text{ s}^{-1}$. (b) Effective bending modulus as a function of shear rate $\dot{\gamma}$. $k_c(\dot{\gamma} = 0) = 22k_B T$.

with σ_1 a reference tension value that does not play any role in the suction experiments at fixed shear rate. This expression, which accurately represents our data, has never been, to our knowledge, theoretically suggested or discussed.

Our results demonstrate that the effect of oscillatory shear flow is to *reduce* membrane fluctuations. This is schematically shown in Fig. 4. In the absence of flow, there is a linear relationship, displayed in the figure as a dashed line, between the relative excess area $(A - A^a)/A^a$ and the logarithm of the tension, $\log[\sigma]$. Note that the fluctuation regime holds only for $\sigma \ll \sigma_0$, and that the extrapolation point $\sigma = \sigma_0$ where fluctuations completely unfold is nonphysical—see, for instance, Refs. [5,8]. The flow excess function $F(\dot{\gamma}, \sigma)$ adds a negative contribution to the relative excess area, thus reducing the amount of membrane area stored in the fluctuations. The slope of this contribution, depicted by the dot-dashed line in the figure, is proportional to shear rate. It holds for $\sigma \gg \sigma_1$. An experiment performed at fixed shear rate will follow the full line in the picture that represents the sum of both contributions. On the other hand, at fixed tension, one moves downwards in the diagram along a vertical line, also reducing the amount of stored area as the shear rate increases. The reference tensions σ_0 and σ_1 do not play any role in a suction experiment that measures only relative excess area differences. On the contrary, the reference tension σ_1 plays a role in the fixed tension experiments, determining the rate at which the shear rate unfolds the fluctuations $\Lambda = \partial\alpha/\partial\dot{\gamma} = \tau_0 \log[\bar{\sigma}/\sigma_1]$, where $\bar{\sigma}$ is the fixed applied tension. The dispersion of the slopes Λ shown in Fig. 2 is therefore the expression of the dispersion in σ_1 , which spans the range $10^{-10} < \sigma_1 < 10^{-5} \text{ Nm}^{-1}$, with most of the values close to $\sigma_1 \sim 10^{-7} \text{ Nm}^{-1}$. The physical origin of σ_0 is well understood [8]. It is formally related to

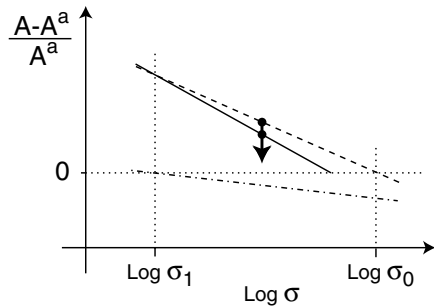


FIG. 4. Helfrich constitutive equation under oscillatory shear flow. Dashed line: linear relation between the relative excess area and the logarithm of the tension without flow. Dotted-dashed line: flow contribution, with a slope proportional to shear rate. Full line: new Helfrich relation, also the trajectory of an experiment at fixed shear rate. Vertical arrow depicts the diagram trajectory for an experiment at fixed tension.

the upper cutoff of the fluctuation spectrum, and thus represents the number of fluctuating modes stored in the vesicle. A dispersion of the values of σ_0 reflects thus variations of the preparation conditions. We argue that σ_1 must be related to the smallest characteristic tension of the membrane, associated with the lower cutoff of the fluctuation spectrum. The dispersion of σ_1 values reflects also inhomogeneities in vesicle formation.

Our results show that the flow perturbs significantly the fluctuations for shear rates $\dot{\gamma}$ larger than a typical shear rate $\dot{\gamma}_0 = \tau_0^{-1}$, with τ_0 of the order of a hundred seconds. This is much larger than the longest relaxation time for vesicle shape fluctuations [15], which is given by the bending time $\tau_K = \eta R_0^3/k_c \sim 0.8$ s for a vesicle of radius $R_0 = 20$ μm . Our results under small amplitude oscillatory flow are quite distinct from the cases of stationary shear flow, where distortion of the vesicle shape has been observed [16] for $\dot{\gamma}\tau_K \gg 1$, and where previous theoretical work [17] has predicted an increase of the fluctuations, with the resulting surface excess being essentially stored in the lower, ellipsoidlike deformation mode. Indeed, within the parameter range corresponding to our working conditions, the flow does not induce any optically discernible deformation of the vesicle but leads to a very significant reduction of fluctuations. Also, our findings are consistent with a linear dependence on shear rate of the relative excess area, different from the quadratic predictions for steady shear flow [17]. In related membrane systems such as smectic lyotropics and sponge phases, suppression of fluctuations has been experimentally reported [18] and theoretically discussed within the framework of phase transitions, as recently reviewed by Marlow and Olmsted [19,20]. For ordered stacks, these effects depend on experimental conditions such as the orientation with respect to the flow or flow gradient directions, or the details of the coupling between hydrodynamic flow and membrane deformation, but share a common feature: fluctuations with average lifetimes

larger than the typical shear rate are convected by the flow and effectively suppressed from the fluctuation spectrum. These predictions lead to characteristic times larger than τ_K by several powers of $k_c/(k_B T)$, and closer to our results. A micropipette rheometer, first designed to inspect the behavior of vesicles under flow, thus appears also as a useful tool to bring new insight to long-standing dynamical issues in statistical physics of soft materials.

This work was supported by the CNRS Chemistry Department under the “Jeunes Equipes” AIP. We thank P. Bassereau and R. Dimova for helpful discussions.

*Present address: Polymer Materials and Engineering Faculty of Applied Sciences, Delft University of Technology (TU Delft), Julianalaan 136, 2628 BL Delft, The Netherlands.

- [1] R. Lipowsky and E. Sackmann, *Structure and Dynamics of Membranes* (Elsevier, Amsterdam, The Netherlands, 1995), Vols. 1A and 1B.
- [2] B. Alberts *et al.*, *Molecular Biology of the Cell* (Garland, New York, 1994).
- [3] D. Lasic, *Nature (London)* **355**, 279 (1992).
- [4] J. van de Pas *et al.*, *Colloids Surf. A* **85**, 221 (1994).
- [5] W. Helfrich, *Z. Naturforsch.* **28c**, 693 (1973).
- [6] S. Safran, *Statistical Thermodynamics of Surfaces, Interfaces and Membranes* (Addison-Wesley, Reading, MA, 1994).
- [7] J.-B. Fournier, A. Ajdari, and L. Peliti, *Phys. Rev. Lett.* **86**, 4970 (2001).
- [8] U. Seifert, *Adv. Phys.* **46**, 13 (1997).
- [9] E. Evans and D. Needham, *J. Phys. Chem.* **91**, 4219 (1987).
- [10] J. Hulin, L. Petit, and C. Matescu, *Physical Hydrodynamics* (Oxford University Press, Oxford, 2001).
- [11] M. Angelowa and D. Imitrow, *Mol. Cryst. Liq. Cryst.* **152**, 89 (1987).
- [12] J.-B. Manneville, P. Bassereau, S. Ramaswamy, and J. Prost, *Phys. Rev. E* **64**, 021908 (2001).
- [13] W. Rawicz *et al.*, *Biophys. J.* **79**, 328 (2000).
- [14] We also took into account standard finite frequency deviations in oscillatory flow, $\dot{\gamma}$ always referring to the effective shear rate at the bottom surface.
- [15] F. Brochard and J. Lennon, *J. Phys. (Paris)* **36**, 1035 (1975).
- [16] K. de Haas *et al.*, *Phys. Rev. E* **56**, 7132 (1997).
- [17] U. Seifert, *Eur. Phys. J. B* **8**, 405 (1999).
- [18] J. Yamamoto and H. Tanaka, *Phys. Rev. Lett.* **74**, 932 (1995).
- [19] S. Marlow and P. Olmsted, *Phys. Rev. E* **66**, 061706 (2002).
- [20] A close inspection of the new constitutive relation reveals that our experimental results cannot be explained by simply introducing a modified, shear rate power law expression for the surface tension. Thus, at this point we were not able to make a working connection with results from Ref. [19] or from elsewhere in the literature.